Title page

i. Title: Adaptation to local climate in size, growth and phenology across 19 silver fir (*Abies alba* Mill.) populations from Switzerland

ii. Running title: Adaptation in size, growth and phenology

iii. Authors: Katalin Csilléry[1,2], Christoph Sperisen[5], Otso Ovaskainen[3,4], Alex Widmer[6], Felix Gugerli[2]

iv. Institutional affiliations:
[1] Department of Evolutionary Biology and Environmental Studies, University of Zürich, Zürich, Switzerland
[2] Biodiversity & Conservation Biology, Swiss Federal Research Institute WSL, Birmensdorf, Switzerland
[3] Department of Biosciences, University of Helsinki, Helsinki, Finland
[4] Centre for Biodiversity Dynamics, Department of Biology, Norwegian University of Science and Technology, Trondheim, Norway
[5] Institute of Integrative Biology, ETH Zürich, Zürich, Switzerland

v. Corresponding author: Katalin Csilléry
Email: katalin.csillery@uzh.ch & kati.csillery@gmail.com

vi. Author contributions: KC designed the study and obtained the SNP data with help from AW and FG. KC performed all analysis with help from OO. CS was involved in the published common garden experiment and provided help with data interpretation. KC wrote the manuscript with help from all other authors.

vii. Acknowledgements: We thank all members of the ADAP project that provided the phenotypic data for this study, especially to Aline Frank, Caroline Heiri and Peter Brang. Additionally, Andrea Kupferschmid helped with correcting some errors in the phenotypic data thanks to her follow up project (EADAPT). Part of the SNP data was provided by FG, and the sampling was conducted by Catherine Folly with the supervision of FG. The project and KC benefited fellowship and a research grant from the Center for Adaptation to a changing environment at the ETH Zürich. We thank Kristian Ullrich for help with the SNP selection, and Dirk Krager with extracting the climatic data from the data bases. The contribution of several field and lab workers was necessary for this project, in particular, we thank René Graf and Olivier Charlandie.

Conflict of Interest Statement: The authors declare no conflicts of interest.

Data archival: SNP data will be archived on dryad.

Adaptation to local climate in size, growth and phenology across 19 silver fir (*Abies alba* Mill.) populations from Switzerland

Abstract

Attempts to identify, understand, and infer selection pressures responsible for local adaptation are central to evolutionary research. Using 19 populations of silver fir sampled across a heterogeneous environment, we tested whether populations have diverged more at quantitative traits than expected from genetic drift. We genotyped at least 20 trees from each population at 374 single-nucleotide polymorphism (SNP) loci to estimate their demographic distances and used these to generate a null expectation for divergence in size, growth and phenology traits obtained from a published garden trial. Further, we used local soil pits and historical climate data to identify the selective environment. Our results revealed a strong selection on height driven by temperature: trees from low-elevation warm sites evolved to become taller than those from cooler high-elevation sites. The evolution of growth rate, duration and bud break were correlated and populations evolved towards two extreme strategies: "start early and grow slow" or "start late and grow fast". The main environmental drivers of evolution towards one or the other strategy were precipitation seasonality. Our results demonstrate that natural selection have shaped the morphology and life-history Swiss silver fir populations. We also identify some populations that may represent suitable seed sources under future climatic conditions.

Keywords:

local adaptation, selection, drift, forest tree, environmental driver, genetic correlation, life-history strategy

Introduction

With increasing concerns about climate change, estimating the adaptive potential of forest trees has high societal and economic relevance. The capacity of many forest tree species to survive and reproduce across a broad geographical range is, at least partly, due to adaptation to local conditions (*e.g.* Aitken *et al.*, 2008; Franks *et al.*, 2014). There is growing evidence that adaptation can be important for enabling populations to persist under changing conditions, including climate change (Hoffmann & Sgrò, 2011). However, many populations are increasingly exposed to novel environmental conditions that are beyond the range to which they are adapted and/or outside of their physiological tolerance (Shaw & Etterson, 2012), and it is unclear how commonly and rapidly adaptations or plastic responses would arise in order to keep up with climate change (*e.g.* Franks *et al.*, 2014).

Many forest tree species have distribution ranges that expand over large geographic regions, which is, at least in the Northern Hemisphere, a result of recent population expansions after the Last Glacial Maximum (Hampe & Jump, 2011). Given the large effective population sizes, predominant outcrossing mode of reproduction, and moderate to high levels of genetic diversity, forest tree species have been able to adapt to local conditions, as reflected by ample empirical evidence of trait divergence patterns that are congruent with south-north climatic gradients (Savolainen *et al.*, 2007; Alberto *et al.*, 2013). However, since many of these gradients also coincide with recent population expansion, it can be difficult to tease apart neutral and selective processes underlying trait variation (*e.g.* Yeaman *et al.*, 2016).

Attempts to identify adaptive trait differentiation in forest trees have often relied on the long tradition of provenance trials, in which different populations from across the geographic range are tested in a common environment. Phenotypic data is often exploited using so-called $Q_{ST} - F_{ST}$ tests, which compare quantitative trait differentiation (Q_{ST}) with genetic divergence inferred from neutral markers (F_{ST}) (Whitlock, 2008; Whitlock & Guillaume, 2009). A recent literature survey of forest trees suggests that most tree traits exhibit considerable heritable trait variation and that Q_{ST} most often (69% of the studies) exceeds F_{ST} (Lind *et al.*, 2018). However, a simple comparison between Q_{ST} and F_{ST} have many

shortcomings that have been criticized (e.g. reviewed in Leinonen *et al.* (2013)), and alternative solutions have been suggested (Chenoweth & Blows, 2008; Martin *et al.*, 2008; Ovaskainen *et al.*, 2011). The fundamental issue is that both Q_{ST} and F_{ST} are random variables, i.e. the observed values are just a single realization of the evolutionary process. Even though Whitlock & Guillaume (2009) proposed an improved $Q_{ST} - F_{ST}$ test where Q_{ST} is compared to a simulated distribution of F_{ST}, this test still does not properly account for the demography, because it is reduced to a single summary of the data, the F_{ST}. Further, the $Q_{ST} - F_{ST}$ test may also give misleading results because each trait in isolation and the signature of adaptive trait differentiation can be the result of selection at another trait if they are genetically correlated (*e.g.* Chenoweth & Blows, 2008). Ovaskainen *et al.* (2011) proposed a novel method, which uses a statistically more powerful null-hypothesis than the $Q_{ST} - F_{ST}$ tests: it takes into consideration the drift distances among all populations (i.e. the coancestry matrix) to derive the null expectation of trait divergence. So far only a handful of applications of this method have been published (*e.g.* De Kort *et al.*, 2016).

Here, we assess adaptive divergence at size, growth and phenology traits in silver fir (*Abies alba* Mill.), an ecologically and economically important European forest tree species. Indeed, recent dendrological (Vitali *et al.*, 2017) and genecological (Frank *et al.*, 2017a) evidence suggest silver fir is potentially better adapted to future climatic conditions, notably to drought, than the other dominant conifer of European forests, Norway spruce (*Picea abies Karst.*). In this study, we concentrate on populations from ecologically diverse sites across Switzerland, including populations from the core range (Central Plateau), but also marginal populations isolated by high mountain ranges. These alpine populations encompass the wet outer Alpine chain to the dry Central Alps across diverse soil types (Ellenberg, 1988). Silver fir populations in Switzerland are rather young, palynological and dynamic vegetation modeling suggest that the Swiss Alps were colonized by silver fir from south to north after the Last Glacial Maximum. The species most likely reached the southern slopes of the Alps between 9 and 10 kyr BP and the northern slopes between 5 and 8 kyr BP (Van der Knaap *et al.*, 2005; Liepelt *et al.*, 2009; Ruosch *et al.*, 2016). Range-wide patterns of chloroplast and mitochondrial DNA variation (Liepelt *et al.*, 2002) and isozyme data (Burga & Hussendörfer, 2001) from extant

silver fir populations suggest that the Swiss Alps were colonized from a single ancestral refugial population situated in the Central or Northern Apennines, even though the potential contribution of eastern refugial populations cannot be excluded.

The potential for adaption can be the greatest in isolated populations and poor environmental conditions, however, gene-flow from the core areas can easily counteract selection (Lenormand, 2002). Many other wind-pollinated conifer species have high levels of gene flow that can be transferred over large distances and elevational gradients (Petit & Hampe, 2006; Kremer *et al.*, 2012). Thus, regardless of the heterogeneous environment across Switzerland, little adaptive trait differentiation is expected among the studied populations. Indeed, results of a large-scale seedling experiment involving 90 silver fir populations across Switzerland show that levels of population divergence are rather low, particularly when compared to those of Norway spruce from the same area (Frank *et al.*, 2017b). For example, population divergence (Q_{ST}) in height for silver fir was 0.22 and in phenological traits ≤ 0.11. Nevertheless, (Frank *et al.*, 2017b) also found that Q_{ST} values of these traits are much higher than population differentiation at isozyme loci ($F_{ST} = 0.034$) in a comparable set of populations (Finkeldey *et al.*, 2000), and speculated that population divergence might reflect adaptation to local environmental conditions. A further evidence for possibly adaptation was that population differentiation in seedling height showed a regional pattern, where seedlings from the Central Plateau were taller than those from the Alps, and environmental variables explained a large proportion of the trait differentiation (49%) (Frank *et al.*, 2017b).

Here, we revisit the phenotypic data obtained by Frank *et al.* (2017b) for a subset of 19 populations, complete it with modern genetic data, and assess to what extent the observed trait differentiation is due to drift or selection. The goal of this study is three-fold. First, we test for adaptive trait divergence using the multi-trait test developed by Ovaskainen *et al.* (2011), thus we account for the full demography in devising the null expectation for trait divergence. Since we have data from a relatively large number of populations and from a highly heterogeneous environment separated by barriers to gene flow, accounting for the likely complex and hierarchical population structure is essential. Further, the studied set of size, growth and phenology traits most likely do not evolve independently, thus the multi-trait approach is

highly desirable to identify any correlated responses to selection. Second, we develop a set of downscaled historical climate variables and adopt soil data from Frank *et al.* (2017b) to test which one of them drives the adaptive divergence patterns using the methodology described in Karhunen *et al.* (2014). Third, we wish to advocate the methodology used herein by proposing this throughly performed case-study, by contrasting the results with the simple $Q_{ST} - F_{ST}$, and proposing two methodological improvements to test for the signature of selection in each population and a more powerful version of the H-test proposed in Karhunen *et al.* (2014).

Material and Methods

Study sites and sampling

In 2009, 90 silver fir stands were selected across Switzerland in the framework of a genecological study (Frank *et al.*, 2017b). From each population, three mother trees were selected from an area with a relief as uniform as possible and with at least 100m distance between them. From this study, we selected a subset of 19 allochthonous populations that represented the main geographic regions of Switzerland (Figure 1A), and re-visited them in 2013 and 2016. In spring 2013, needles were sampled from nine to ten adult trees, including the three mother trees, if they were found. In spring 2016, needles were sampled from an additional ten to twelve trees, always respecting a minimum distance of 100m between the newly or previously sampled trees. In total, 387 adult trees were used in this study, with at least 20 individuals per population. Needles were stored in plastic bags for a maximum of one week at $5°C$ before being freeze-dried and prepared for DNA extraction.

Genetic data

All adult trees were genotyped at 374 single-nucleotide polymorphism (SNP) originating from three different sources. First, we used SNPs discovered from 13 *A. alba* trees originating from Mont Ventoux (France) and the Black Forest (District Oberharmersbach, Germany). Transcriptomes were sequenced on an Illumina HiSeq2000 at IGA Technology Services (Udine, Italy). Transcriptome assembly and SNP detection was carried out with an in-house

pipeline at IGA; see details in Roschanski *et al.* (2013). Previous SNP genotyping using a KASP array manufactured by LGC Genomics (Middlesex, United Kingdom) in French populations yielded 267 polymorphic loci situated in 175 different candidate genes (Roschanski *et al.*, 2016). In this study, 220 of these loci were successfully genotyped using the same KASP array. Second, we selected 110 new putatively neutral SNPs from the transcriptom assembly based on their Tajima's D being between 2 and -2 and dN/dS between 0.9 and 1.1, low LD with the existing 224 SNPs (r2 < 0.1 and p-values > 0.05). ESTScan version 3.0.3 (Iseli *et al.*, 1999) for *Arabidopsis thaliana* was used to predict coding DNA sequences for each contig from the transcriptome (Roschanski *et al.*, 2013), then the SNPs detected by IGA were used to create pseudo-contigs on which the neutrality statistics were calculated. dN/dS was calculated with 'polydNdS'[1] based on (Thornton, 2003), and Tajima's D with VariScan v2.0.3 (Vilella *et al.*, 2005). Although all 110 SNPs passed initial in silico design tests, only 25 of these SNPs were successfully genotyped on a KASP array, most likely because the primer sequences were not specific enough (results not shown). Third, we selected 149 SNPs from Mosca *et al.* (2012), who discovered SNPs by resequencing 800 amplicons using PCR primer pairs from *Pinus taeda* in 12 *Abies alba* trees, and genotyped on a Golden Gate platform (Illumina, San Diego, CA, USA). We selected SNPs from this study that had less than 5% missing data. 129 of these SNPs were successfully genotyped on a KASP array. Both DNA extraction and all genotyping was performed using the all-inclusive service from LGC Genomics (Middlesex, United Kingdom).

Common garden experiment

We used published seedling phenotype data from the descendants of three mother trees from each of the 19 populations (Frank *et al.*, 2017b), while correcting inconsistencies and outliers based on measurements taken in subsequent years (unpublished data of Andrea Kupferschmid). For the sake of completeness, we briefly summarize the protocol of the experiment relevant for silver fir. In April 2010, from each mother tree (subsequently called family) approximately 2000 seeds were sown directly into nursery beds and grown for two

[1] `https://github.com/molpopgen/analysis`

years at the Swiss Federal Research Institute WSL in Birmensdorf, Switzerland ($47°21'42''N$, $8°27'22''E$, 550 m elevation). Families and populations were not replicated or randomized in the nursery. In spring 2012, a random selection of at least 12 viable seedlings per family were transplanted with present terminal buds to the open experimental field site. The field site was located at Brunnersberg, a former pasture on a south facing slope (20-24% incline) in the Swiss Jura Mountains ($47°19'35''N$, $7°36'42''E$, 1090 m elevation). Seedlings were planted at 30×40 cm spacing in 10 blocks. Provenances, families and seedlings were randomized across blocks. Mortality during 2012 in the field was minor. Seedling height and diameter were measured in the autumn of 2012 and used in the analysis as a covariate to account for possible growth differences in the nursery.

Phenotypic measurements used herein were performed in spring and autumn of 2013. Measurements of seedling height and Terminal and Lateral Bud Break started on 7 May 2013, when the first seedlings started to break buds, i.e. the membrane below bud scales was broken and the first green needles became visible. Observations of bud break dates continued twice a week until Growth Cessation, defined as the date when 95% of terminal leader height growth was achieved. 5 to 17 height measures were recorded per seedling from which a Maximum Growth Rate was calculated as the first derivative of the growth curve (subsequently called Growth Rate, for simplicity). Growth Duration was calculated as time from Terminal Bud Break to Growth Cessation. Final seedling Height from ground surface to the uppermost bud base and stem Diameter at two cm above ground surface were measured in autumn 2013. Finally, we also calculated the ratio Height/Diameter to test for trait divergence in growth allometry. For clarity, we call Height, Diameter, Height/Diameter size traits, Growth Rate and Duration growth traits, and the two Bud Break and Growth Cessation (equivalent to bud set) phenology traits. All traits were normally distributed and correlated with one another to a varying extent (see Figure S1).

Environmental data

We used soil characteristics and downscaled historical climatic data to characterize environmental conditions in each population. Soil and geographic variables were adopted from

Frank *et al.* (2017b), who established soil pits within a few meters of one of the mother trees (see list of variables used in Table S1). In order to obtain the closest representation of the climate of the period when the current populations were established, we used data from 1 January 1901 to 31 December 1978. The choice of this period was justified by two facts: (i) no observation-based climate data go back further in time, and (ii) starting from approximately 1980, the temperature time series are overwhelmed by the effect of global warming (Harris *et al.*, 2014). We used statistical downscaling using the delta method (Hay *et al.*, 2000) to obtain 1 km grid scale mean monthly temperature and precipitation fields for this period. The reference climatic data set was the $0.5°$ resolution CRU TS v. 4.01 data (20 September 2017 release, Harris *et al.* (2014)) available for the 1 January 1901 - 31 December 2016 period, while the downscaling was based on the overlapping period of 1 January 1979 - 31 December 2016 with the 1 km resolution Chelsa data (Karger *et al.*, 2017).

We calculated several bioclimatic indexes to characterize the environment for each site, including the 19 bioclimatic variables (Booth *et al.*, 2014) implemented in the R package dismo (Hijmans *et al.*, 2017), two potential evapotranspiration (PET) indexes and four standardized precipitation - evapotranspiration index (SPEI) variables using the R package SPEI (Beguería & Vicente-Serrano, 2017), and two indicators of late frost (Table 1). Soil available water capacity (AWC) was obtained at a 250 m resolution from the Soilgrids data base (Hengl *et al.*, 2017). Using temperature, precipitation and AWC, we calculated the self-calibrated Palmer's drought severity index or scPDSI (Wells *et al.*, 2004), and summarized to measures of drought severity and frequency across the full time series (Table 1). All climatic variables were considered as raw values or as deviations from the common garden environment in Brunnersberg (based on the Chelsa data for the period of 1 January 1979 - 31 December 2013). However, the two ways of calculating the climate led to the same conclusions (results not shown), so we present results with the raw variables only for ease of interpretation. To visualize the environmental differences between sites, we conducted a Principal Component Analysis (PCA) of all environmental variables of Tables 1 and S1, scaled and centered to make them comparable. The first PCA explained 32.6% of the variance and was dominated by temperature variables, and the second PCA axis explained 18.8% of the

variance and was dominated by precipitation variables (Figure S2).

Statistical analysis

We used both single-trait and multi-trait approaches to test if the phenotypic divergence between populations is due to selection. First, we used a single-trait $Q_{ST} - F_{ST}$ test using the bootstrap procedure described in Whitlock & Guillaume (2009) implemented in the R package QstFstComp (Gilbert & Whitlock, 2015)[2]. We considered a one-tailed test, because we were interested in testing for adaptive divergence only, thus Q_{ST} being significantly greater than F_{ST}. Second, we used single- and multi-trait versions of the test of adaptive divergence (S-test) developed by (Ovaskainen *et al.*, 2011) and implemented in the R package driftsel[3]. We estimated the coancestry matrix between all pairs of populations from variation in SNP allele frequencies based on the admixture F-model (AFM) using a Metropolis-Hastings algorithm implemented in the R package RAFM[4] (Karhunen & Ovaskainen, 2012). Thus, we assumed that contemporary populations evolved from a single ancestral population, which is likely a reasonable assumption for silver fir in Switzerland (Liepelt *et al.*, 2002; Burga & Hussendörfer, 2001). Ten independent Markov chains of the AFM model reached slightly different local optima using a burn-in of 20,000 iterations followed by 10,000 iterations for estimation with a thinning interval of ten. Running longer chains (up to 50,000 iterations tested, results now shown) did not improve convergence to a common optimum, so we averaged the posterior distributions across the ten chains. Further, to gain more confidence in the estimated coancestry matrix, we compared the averaged coancestry matrix against that estimated using Bayesian clustering algorithm implemented in the software Structure v.2.3.4 Pritchard *et al.* (2000) (see Supporting Information for more details). Third, we used the H-test, developed by Karhunen *et al.* (2014), and a standardized version of it, subsequently referred to H^*, to identify the potential environmental drivers of local adaptation. In the following paragraphs, we briefly summarize the rationale of the S-test, and its population-wise

[2] `https://github.com/kjgilbert/QstFstComp`

[3] `https://www.helsinki.fi/en/researchgroups/metapopulation-research-centre/rafm-and-driftsel`

[4] `https://www.helsinki.fi/en/researchgroups/metapopulation-research-centre/rafm-and-driftsel`

version, proposed herein, and the rationale of the proposed H^* statistic.

When populations are derived from a common ancestral population, the matrix of population-level additive effects A under drift is expected to be distributed as multivariate normal (MNV) (Ovaskainen *et al.*, 2011):

$$A \sim MVN(\mu \otimes I, 2G^A \otimes \theta),$$

where μ is the mean additive genotype in the ancestral population, which is determined by the allele frequencies in the ancestral population, I is the identity matrix relating individuals to populations, G^A is the ancestral variance-covariance matrix of the traits in question, θ is the matrix of population-level coancestry (estimated using AFM), and $\otimes$ is the Kroenecker product. Ovaskainen *et al.* (2011) proposed to use a Bayesian mixed-effects animal model to co-estimate μ and G^A while accounting for the family structure of the common garden (i.e. the pedigree) and θ. The S-test is based on the S statistic calculated as the mean Mahalanobis distance between the mean additive trait values in the contemporary populations from the mean ancestral trait value. $S = 0.5$ indicates consistency with neutrality, $S = 0$ implies a match with purifying, and $S = 1$ with diversifying selection. Thus, S measures the overall signature of selection across all populations. In this study, we propose to test if any particular populations show significant trait divergence, which can be particularly useful when the number of populations is great (e.g. > 5). Indeed, a single S statistic cannot distinguish between the two scenarios of many populations that are slightly diverged or a single/few populations that are diverged to great extent. In a single trait context, the population-wise S statistic is significant if the population's estimated additive trait value is smaller or larger than the 0.025% or 0.975% percentiles of that under drift. In a two-trait context, the critical value for each population is an ellipse that contains 95% of additive genetic trait space under drift.

The H statistics measure if the distance between the populations' mean additive trait values is more similar to the environmental distances than expected based on drift (Karhunen *et al.*, 2014). The original H-test is based on the Mantel test statistic, i.e. the product moment between the distance matrices of environment and traits. As the covariance is not only influenced by the

correlation between the matrices but also by the absolute values of trait differences, the original H-test may yield false positive results. In particular, where there is strong evidence for selection, the H statistic can be maximal (i.e. $H = 1$) even when the selection is uncorrelated with the tested environmental driver. For this reason, we propose the use of the H^* statistic, which is the Pearson or standardized Mantel statistic, thus the H^*-test can be viewed as a standardized version of the H-test. We note that the superiority of a standardized Mantel statistic has already been pointed out in the context of spatial distance matrices (Legendre & Fortin, 2010). The population-wise S-test and the H^*-test are now implemented in the most recent version of the R package driftsel.

Results

Population structure and drift distances

F_{ST} using the Whitlock & Guillaume (2009) approach was 0.006 (95% confidence interval: 0.002, 0.1015). The drift distances estimated with AFM indicated the presence of two main clusters that correspond to eastern and western populations (Figure 1B). The population POS did not belong to either of these groups, which is plausible given that it is situated south of a high mountain pass (the Bernina pass) close to the Italian border (Figure 1A). The coancestry matrix can also be used to obtain a coancestry-based estimate the F_{ST}, which was 0.0184 (95% credible interval: 0.0167, 0.0202) for the 19 populations. The comparison between AFM and Structure revealed similar results yet suggested that AFM is more flexible to reveal the complex hierarchies in the population structure (see Supporting Information for more details).

Single trait analysis

Single trait tests of adaptive divergence in terms of $Q_{ST} - F_{ST}$ comparisons using the Whitlock & Guillaume (2009) approach and in terms of the S statistic from the Ovaskainen *et al.* (2011) method gave similar results (Table 2). Using either of the methods, the strongest signature of adaptive divergence was observed for seedling Height followed by four other traits with a strong evidence of selection; in decreasing order of evidence based on the S statistic: Lateral

Bud Break, Terminal Bud Break, Diameter, and Growth Duration. The remaining three traits showed no or weak signal of unusual trait differentiation using either of the approaches. For Growth Cessation and Height/Diameter the $Q_{ST} - F_{ST}$ test was marginally significant, while the S statistic was close to 0.5. For Growth Rate, there was no evidence of selection using either approach.

The population-wise S-tests revealed a signature of selection in several populations. Figure 2 shows, for each trait, how much each population diverged from the ancestral mean (horizontal line) and if this divergence is more than expected by drift (i.e. if boxes extend beyond the gray envelope). These population-level estimates confirmed that Height diverged the most among populations (Figure 2B): eight out of 19 populations significantly deviated from the neutral expectations (indicated by the stars above the boxes). All these eight populations evolved towards a higher mean height and no populations have been selected for reduced height. Although the population-wise S-test was not significant for any in the populations for Diameter, the first seven tallest populations also had the largest Diameter (Figure 2A), suggesting co-evolution between Height and Diameter and explaining the lack of unusual differentiation at Height/Diameter (Figure 2C). Significant trait divergence was also observed for a single individual population, SIR, for Growth Duration (Figure 2E) and Lateral Bud Break (Figure 2H). The SIR population evolved towards earlier bud break and longer growth duration than expected by drift alone. At the opposite end of the trait space, population VRG evolved towards late Terminal Bud Break and shorter Growth Duration, yet its divergence level was not significant in this single trait test.

Multi-trait analysis

We performed only two trait analysis due to convergence problems with three of more traits (results not shown). For simplicity, we considered only one of the bud break traits in this pairwise analysis, the Terminal Bud Break, because the two traits were very strongly correlated. The additive genetic variance and covariances for all traits and trait pairs, respectively, were calculated as $2G^A(1 - \theta_X)$, where G^A is the ancestral variance-covariance matrix and θ_X is the diagonal of the coancestry matrix. Then, the heritabiliy of each trait and

the genetic correlation all between trait pairs were calculated as the proportion of the phenotypic variance and covariances that are additive (Falconer & Mackay, 1996). The heritabilities reported in Table S2 are slightly different for a given trait depending on the particular pairwise analysis because the G^A is different and also the θ matrix is updated when the population effects are estimated. For most trait pairs the genetic correlations were small or negligible (Table S2) and agreed well with phenotypic correlations (Figure 3A). The highest phenotypic correlation (0.64) was observed between size traits, between Height and Diameter, yet their genetic correlation was half as much (0.32, Table S1). Figure 4 shows the effect of selection on these two traits. The ellipses illustrate the drift distances of each population from the ancestral trait value (indicated by the letter A) based on neutral processes only. The population names are placed at the estimated current population means, so the further they are from the ellipses, the more selection has pushed them towards a particular phenotype. Ten populations showed significant divergence, their ellipses and population names are in black (Figure 4). In contrast, some unusually high genetic correlations (i.e. higher than the phenotypic equivalents) were observed between traits of different kind: between growth and phenology (Growth Duration and Terminal Bud Break, between Growth Rate and Terminal Bud Break), and between size and phenology (Height/Diameter and Growth Cessation, see Figure 3A). However, the S statistics was high for the first two trait pairs (Figure 3B), suggesting a correlated evolution at the three traits. Figure 5 shows that for each trait pair, two populations reached a significant level of divergence in the opposite directions. The easiest way to think about these diverged populations is in terms of life-history strategies. SIR is significantly diverged in all three trait combinations, along with MGY, even though the latter reached the significance level only for Growth Duration vs Growth Rate (Figure 5). For simplicity, we can say that SIR and MGY follow a "start early and go slow" strategy, i.e. they burst buds early and then grow for a long time at a low rate. At the other end of trait space, population VRG follows a "start late and run" strategy, i.e. bursts buds late, but then grows fast for a short period of time (Figure 5).

Environmental drivers

H and H^* assess how much each environmental variable moves the Mantel statistic away from the neutral expectation (i.e. random association with the environment conditional on the drift distances). Table 2 shows the H and H^* statistics for each trait when using information from all environmental variables listed in Tables 1 and S1 (subsequently referred to global environment). The global environment explained trait divergence for Diameter, Height and Growth Rate (Table 2). For traits where S was close to 0.5, such as Height/Diameter and Growth Cessation, adding the environmental variables only added noise. Similarly, for Bud Break traits and Growth Duration, H was also slightly smaller than S and H^* was close to 0.5 (Table 2). However, using the global environment, we assume that all aspects or the dominant aspect of the environment, which is the temperature (Figure S2), matter for adaptation. In reality, it is likely that for each particular trait a particular aspect of the environment matters more than other aspects, so we applied the H and H^* tests for each environmental variable listed in Tables 1 and S1 separately. Since our objective was to prioritize the environmental variables, we did not correct for multiple testing. Figure 6 illustrates the difference between the H and H^* statistics. The two statistics generally correlate well, but it is apparent that the H^* statistic has more discriminatory power, especially for traits under strong selection, such as Height, where H was one for all environmental variables (Figure 6).

The role of the environment in the divergence of Height and Diameter was most important among all traits (Table 2, Figure 6). Additionally, the environmental variables that had an H^* statistic higher than 0.95 for Height included all variables that fulfilled the same criteria for the Diameter, suggesting that the same environmental cues matter for the evolution of both traits. Remarkably, all of these environmental variables were related to temperature and drought, but not precipitation per se. The most important environmental variables in the order of decreasing H^* statistic for Height were Thornthwaite's mean annual evapotranspiration (PET.thorn), mean temperature of the warmest quarter (bio.10), isothermality (bio.3), annual mean temperature (bio.1), available water capacity (AWC), elevation, mean temperature of the coldest quarter (bio.11), maximum temperature of the warmest month (bio.5), minimum temperature of the coldest month (bio.6), mean diurnal range (bio.2), latitude and drought

severity measured as the 1% quantile of the self-calibrated Palmer's Drought Severity Index across the whole time series. To support the interpretation of these results, we performed a PCA of these environmental variables. Figure 7A illustrates that all populations that diverged towards a bigger size in terms of Height and Diameter were situated at the warm, stable and humid side of the environmental space. Finally, note that the precipitation-related variables (bio.12, bio.13, bio.14, bio.15, bio.18) had the lowest correlation with adaptive divergence for tree size (H^*-statistics were below 0.5).

Divergence at the two Growth traits and at the two Bud Break traits also correlated with habitat differences: the most important environmental variables ($H^* \geq 0.85$) largely overlapped for these traits and were most often related to precipitation (Figure 7B). Mean temperature of the wettest quarter (bio.8), precipitation seasonality (bio.15), precipitation of warmest quarter (bio.18), and mean diurnal range (bio.2) were omnipresent as environmental variables with the highest H^*-statistics for the four traits. Again, the common habitat variables that explain adaptation for these traits is not surprising given the evidence for their correlated evolution (Figure 5). The PCA of these environmental variables illustrates that the drivers of the "start early and go slow" strategy of SIR, and to some extent that of MGY and GRY, are low average precipitation, lack of precipitation seasonality, and high temperature amplitude both at the annual and monthly levels (Figure 7B), reflecting the cold winters and hot and dry summers of the Rhône Valley. At the other end of the trait space, the climate of population VRG is characterized by ample winter precipitation, late snow and late frost, and low soil silt content, which could explain the late bud break and short but fast growth of this population (Figure 7B).

Discussion

In this study, we found clear evidence of local adaptation at size, growth and phenology traits across 19 Swiss silver fir populations. Three size (Height and Diameter) has been under strong selection in warm and humid areas of Switzerland (Central Plateau), where populations evolved towards a taller and larger stature (Figure 4 and 7). The role of selection on Height is further supported by the fact that the selection gradient is south-north (northern populations being taller), while the main demographic axes is east-west (Figure 1B). The annual

development cycle of temperate trees result from an evolutionary trade-off between two opposing forces: maximizing the length of the vegetative season while avoiding late frost and summer drought. This life-history decision is particularly crucial in mountainous environments, where the length of the growing season is often limited. In thus study, the timing, the rate, and the duration of growth have been under selection pressure that allowed populations to evolve towards two extreme strategies that reflect adaptation to the amount and timing of the precipitation (Figure 5 and 7). Populations of the Rhône Valley, especially SIR, but also MGY, GRY (Figure 1A), seem to persevere the conditions of this notoriously dry inner Alpine valley of Switzerland. Here, annual precipitation is low and falls mainly in winter, while high temperatures and drought are common during spring and summer. These populations are adapted to such climatic conditions through early bud break and slow growth during the dry but long vegetative season (Figure 5). We observed the opposite strategy in VRG, and to some extent in MUO. Both populations are situated in high-altitude mountain valleys (Figure 1A), where late snow delays the start of the vegetative season, but then growth is fastest in these populations (Figure 5).

Quantitative genetic theory suggests that fitness-related traits are under strong selective pressure with stabilizing selection reducing genetic variation among individuals (*e.g.* Mousseau & Roff, 1987). As a result, it is often observed that heritability estimates are lower on morphological than on life-history traits (Visscher *et al.*, 2008). In contrast, estimates of the heritability from Frank *et al.* (2017b) using 90 populations revealed the highest heritability for the phenology and growth, and lowest for size. Further, our estimates of the heritability derived from the ancestral G-matrix also revealed the highest values for the two Bud Break traits, while the lowest for Height (Table S2). We may speculate that Height have been under strong selection, thus its additive genetic variance have been reduced. The fitness advantage of being tall for trees are clear, since a high stature facilitates the pollen and grain dispersion (Petit & Hampe, 2006). Further, artificial selection for height may also have affected these populations, further reducing the additive genetic variance. The populations that have been selected for taller height in this study (Figure 2B) are located in the geographic region that are the most easily accessible for foresters due to their low elevation and flat terrain. Since tree

height is a key trait from an economical point of view and there has been a long history of management in this region (*e.g.* Bürgi & Schuler, 2003), we cannot exclude the possibility that there has been artificial selection in these populations.

Interestingly, two traits, Height/Diameter and Growth Cessation, did not show evidence of adaptive divergence, but they were genetically correlated (0.25), while lacking any phenotypic correlation (0.04, Figure 3, Table S1). The allometric relationship between Height and Diameter has been extensively studied in forest trees because it determines the volume of the harvestable stem and carbon storage and it is also associated with wood quality such as lignin and cellulose content (*e.g.* Chave *et al.*, 2014). The fact that Growth Cessation did not show a signature of selection may seem surprising given the overwhelming evidence of adaptive clines for bud set (a proxy for growth cessation) at many species, including conifers (Alberto *et al.*, 2013). The explanation may lie in the deterministic bud development of the *Abies* species (Cooke *et al.*, 2012). They produce terminal buds during the summer at the tip of each leading branch shoot and remains dormant during the following winter. Each bud contains a preformed miniature of the terminal and lateral shoots with all the needles that will grow to branches and photosynthesizing needles during the following growing season. Thus, given that the timing of the start (bud burst) and the rate (maximum growth rate and growth duration) of this developmental trait have been under selection selection (Figure 5), the timing of the end cannot be under selection. The positive genetic and negligible phenotypic correlation between Height/Diameter and Growth Cessation may indicate the trees can only increase their Height in relation to their Diameter at the price of growing longer, however, the evolution of this developmental process is extremely constrained due to canalization.

A long-standing hypothesis in evolutionary biology is that traits belonging to the same functional and/or developmental group are genetically more integrated than traits with different functions or developmental origins (Berg, 1960; Pigliucci & Preston, 2004). Several empirical studies found evidence that there is greater genetic and phenotypic character integration within suites of functionally or developmentally related traits than between them, e.g. between and within floral vs. vegetative traits in plants (Waitt & Levin, 1998; Baranzelli *et al.*, 2014). In this study, we measured exclusively vegetative traits, but three kinds, related to

size, to growth, and to phenology. Indeed, we found that the genetic correlations tended to be higher than phenotypic correlations between different trait kinds than within (Figure 3A), and in particular, between growth and phenology. These results suggest that at the physiological and molecular level, growth and phenology are strongly linked.

Overall our methodology proved more informative than classical $Q_{ST} - F_{ST}$ comparisons, even though the high number of populations leveraged the power of the classical test and led to similar global conclusions (Table 2). First, we were able to pinpoint which populations diverged significantly from a supposed ancestral trait value (Figure 2). Second, the multi-trait analysis allowed us to identify life-history strategies that are under selection, and third, we were able to identify the selective environment. In particular, we found that the same environmental variables explained best the single-trait adaptive population differentiation at traits that were genetically correlated in the multi-trait analysis, which provides particularly strong evidence for the role of temperature and humidity in the evolution of tree size (Figure 7A) and the role of precipitation seasonality in the timing and mode of growth (Figure 7B).

Recent evidence suggests a global increase in climate-driven forest decline that is primarily driven by a combination of rising temperatures and drought stress, so-called hot-drought, e.g. Allen *et al.* (2010). Such conditions foster detrimental agents such as pests (pathogens, herbivores) or physical disturbances such as storms (*e.g.* Csilléry *et al.*, 2017). For Europe, the most recent IPCC report predicts an increase in temperature, along with a decrease in summer precipitation and an increase in winter precipitation (Stocker *et al.*, 2014). Although there is abundant evidence of the past evolution of plants in response to climate, such as past range shifts during glaciations (*e.g.* Kawecki & Ebert, 2004; Aitken *et al.*, 2008), the question is the extent to which adaptive evolution can compensate the effects of rapid climate change. Silver fir may already be in danger in some areas of the Mediterranean, where die-back events have been documented (Cailleret *et al.*, 2014), or in south-western Europe, where reduced growth patterns have been reported (Gazol *et al.*, 2015). Yet, positive effects of climate warming have also been observed in temperate areas, where warming enhanced growth (Gazol *et al.*, 2015). The predicted pace of climate change is much faster than it has been during the time since post-glacial expansion/re-colonization, thus assisted migration can provide a practical solution

(Aitken & Bemmels, 2015). Based on our results, populations of the Rhône Valley may provide dry tolerant seed sources for future plantations in other parts of Switzerland.

References

Aitken SN, Bemmels JB (2015) Time to get moving: Assisted gene flow of forest trees. *Evolutionary Applications*, pp. n/a–n/a. doi:10.1111/eva.12293.

Aitken SN, Yeaman S, Holliday JA, Wang T, Curtis-McLane S (2008) Adaptation, migration or extirpation: climate change outcomes for tree populations. *Evolutionary Applications*, **1**, 95–111. doi:10.1111/j.1752-4571.2007.00013.x.

Alberto FJ, Aitken SN, Alía R, *et al.* (2013) Potential for evolutionary responses to climate change - evidence from tree populations. *Global Change Biology*, **19**, 1645–1661. doi: 10.1111/gcb.12181.

Allen CD, Macalady AK, Chenchouni H, *et al.* (2010) A global overview of drought and heat-induced tree mortality reveals emerging climate change risks for forests. *Forest Ecology and Management*, **259**, 660–684. doi:10.1016/j.foreco.2009.09.001.

Baranzelli MC, Sersic AN, Cocucci AA (2014) The search for pleiades in trait constellations: functional integration and phenotypic selection in the complex flowers of *Morrenia brachystephana* (*Apocynaceae*). *Journal of Evolutionary Biology*, **27**, 724–736.

Beguería S, Vicente-Serrano SM (2017) SPEI: calculation of the standardised precipitation-evapotranspiration index. *R package version 1.7*, **1**.

Berg R (1960) The ecological significance of correlation pleiades. *Evolution*, **14**, 171–180.

Booth TH, Nix HA, Busby JR, Hutchinson MF (2014) Bioclim: the first species distribution modelling package, its early applications and relevance to most current maxent studies. *Diversity and Distributions*, **20**, 1–9.

Burga CA, Hussendörfer E (2001) Vegetation history of *Abies alba* mill.(silver fir) in switzerland–pollen analytical and genetic surveys related to aspects of vegetation history of *Picea abies* (L.) H. Karsten (Norway spruce). *Vegetation History and Archaeobotany*, **10**, 151–159.

Bürgi M, Schuler A (2003) Driving forces of forest management - an analysis of regeneration practices in the forests of the swiss central plateau during the 19th and 20th century. *Forest ecology and management*, **176**, 173–183.

Cailleret M, Nourtier M, Amm A, Durand-Gillmann M, Davi H (2014) Drought-induced decline and mortality of silver fir differ among three sites in Southern France. *Annals of Forest Science*, **71**, 1–15. doi:10.1007/s13595-013-0265-0.

Chave J, Réjou-Méchain M, Búrquez A, *et al.* (2014) Improved allometric models to estimate the aboveground biomass of tropical trees. *Global change biology*, **20**, 3177–3190.

Chenoweth SF, Blows MW (2008) q_{ST} meets the G matrix: The dimensionality of adaptive divergence in multiple correlated quantitative traits. *Evolution*, **62**, 1437–1449. doi:10.1111/j.1558-5646.2008.00374.x.

Cooke JE, Eriksson ME, Junttila O (2012) The dynamic nature of bud dormancy in trees: environmental control and molecular mechanisms. *Plant, Cell & Environment*, **35**, 1707–1728.

Csilléry K, Kunstler G, Courbaud B, Allard D, Lassègues P, Haslinger K, Gardiner B (2017) Coupled effects of wind-storms and drought on tree mortality across 115 forest stands from the Western Alps and the Jura mountains. *Global Change Biology*. doi:10.1111/gcb.13773.

De Kort H, Vander Mijnsbrugge K, Vandepitte K, Mergeay J, Ovaskainen O, Honnay O (2016) Evolution, plasticity and evolving plasticity of phenology in the tree species Alnus glutinosa. *Journal of Evolutionary Biology*, **29**, 253–264. doi:10.1111/jeb.12777.

Earl DA, *et al.* (2012) Structure harvester: a website and program for visualizing structure output and implementing the evanno method. *Conservation genetics resources*, **4**, 359–361.

Ellenberg H (1988) *Vegetation ecology of central Europe*. Cambridge University Press, Cambridge, UK.

Evanno G, Regnaut S, Goudet J (2005) Detecting the number of clusters of individuals using the software structure: a simulation study. *Molecular ecology*, **14**, 2611–2620.

Falconer DS, Mackay TFC (1996) *Introduction to Quantitative Genetics*. Longmans Green, Harlow, Essex, UK, 4 edn.

Falush D, Stephens M, Pritchard JK (2003) Inference of population structure using multilocus genotype data: linked loci and correlated allele frequencies. *Genetics*, **164**, 1567–1587.

Finkeldey R, Mátyás G, Sperisen C, Bonfils P (2000) Strategien zur auswahl forstlicher genreservate in der schweiz. *Forest Snow and Landscape Research*, **75**, 137–152.

Frank A, Howe GT, Sperisen C, Brang P, Clair JBS, Schmatz DR, Heiri C (2017a) Risk of genetic maladaptation due to climate change in three major European tree species. *Global Change Biology*, pp. 1–14. doi:10.1111/gcb.13802.

Frank A, Sperisen C, Howe GT, Brang P, Walthert L, Clair JBS, Heiri C (2017b) Distinct genecological patterns in seedlings of Norway spruce and silver fir from a mountainous landscape. *Ecology*, **98**, 211–227. doi:10.1002/ecy.1632.

Franks SJ, Weber JJ, Aitken SN (2014) Evolutionary and plastic responses to climate change in terrestrial plant populations. *Evolutionary Applications*, **7**, 123–139. doi:10.1111/eva.12112.

Galili T (2015) dendextend: an r package for visualizing, adjusting, and comparing trees of hierarchical clustering. *Bioinformatics*. doi:10.1093/bioinformatics/btv428.

Gazol A, Camarero JJ, Gutiérrez E, *et al.* (2015) Distinct effects of climate warming on populations of silver fir (*Abies alba*) across europe. *Journal of Biogeography*, **42**, 1150–1162.

Gilbert KJ, Whitlock MC (2015) $q_{ST} - -f_{ST}$ comparisons with unbalanced half-sib designs. *Molecular ecology resources*, **15**, 262–267.

Hampe A, Jump AS (2011) Climate relicts: past, present, future. *Annual Review of Ecology, Evolution, and Systematics*, **42**.

Harris I, Jones P, Osborn T, Lister D (2014) Updated high-resolution grids of monthly climatic observations–the cru ts3. 10 dataset. *International Journal of Climatology*, **34**, 623–642.

Hay LE, Wilby RL, Leavesley GH (2000) A comparison of delta change and downscaled gcm scenarios for three mountainous basins in the united states. *JAWRA Journal of the American Water Resources Association*, **36**, 387–397.

Hengl T, de Jesus JM, Heuvelink GB, *et al.* (2017) Soilgrids250m: Global gridded soil information based on machine learning. *PLoS one*, **12**, e0169748.

Hijmans RJ, Phillips S, Leathwick J, Elith J, Hijmans MRJ (2017) Package 'dismo'. *Circles*, **9**.

Hoffmann AA, Sgrò CM (2011) Climate change and evolutionary adaptation. *Nature*, **470**, 479–485.

Hubisz MJ, Falush D, Stephens M, Pritchard JK (2009) Inferring weak population structure with the assistance of sample group information. *Molecular Ecology Resources*, **9**, 1322–1332. doi:10.1111/j.1755-0998.2009.02591.x.

Iseli C, Jongeneel CV, Bucher P (1999) ESTScan: a program for detecting, evaluating, and reconstructing potential coding regions in EST sequences. In: *ISMB: International Conference on Intelligent Systems for Molecular Biology*, vol. 99, pp. 138–148.

Jakobsson M, Rosenberg NA (2007) CLUMPP: a cluster matching and permutation program for dealing with label switching and multimodality in analysis of population structure. *Bioinformatics*, **23**, 1801–1806.

Karger DN, Conrad O, Böhner J, *et al.* (2017) Climatologies at high resolution for the earth's land surface areas. *Scientific data*, **4**, 170122.

Karhunen M, Ovaskainen O (2012) Estimating population-level coancestry coefficients by an admixture F model. *Genetics*, **192**, 609–617. doi:10.1534/genetics.112.140871.

Karhunen M, Ovaskainen O, Herczeg G, Merilä J (2014) Bringing habitat information into statistical tests of local adaptation in quantitative traits: A case study of nine-spined sticklebacks. *Evolution*, **68**, 559–568. doi:10.1111/evo.12268.

Kawecki TJ, Ebert D (2004) Conceptual issues in local adaptation. *Ecology Letters*, **7**, 1225–1241. doi:10.1111/j.1461-0248.2004.00684.x.

Kremer A, Ronce O, Robledo-Arnuncio JJ, *et al.* (2012) Long-distance gene flow and adaptation of forest trees to rapid climate change. *Ecology Letters*, **15**, 378–392. doi: 10.1111/j.1461-0248.2012.01746.x.

Legendre P, Fortin MJ (2010) Comparison of the mantel test and alternative approaches for detecting complex multivariate relationships in the spatial analysis of genetic data. *Molecular ecology resources*, **10**, 831–844.

Leinonen T, Mccairns RJS, Hara RBO, Merilä J (2013) $Q_{ST}--F_{ST}$ comparisons: evolutionary and ecological insights from genomic heterogeneity. *Nature Reviews Genetics*. doi:10.1038/nrg3395.

Lenormand T (2002) Gene flow and the limits to natural selection. *Trends in Ecology & Evolution*, **17**, 183–189.

Liepelt S, Bialozyt R, Ziegenhagen B (2002) Wind-dispersed pollen mediates postglacial gene flow among refugia. *Proceedings of the National Academy of Sciences*, **99**, 14590–14594.

Liepelt S, Cheddadi R, de Beaulieu JL, *et al.* (2009) Postglacial range expansion and its genetic imprints in *Abies alba* (Mill.) - A synthesis from palaeobotanic and genetic data. *Review of Palaeobotany and Palynology*, **153**, 139–149. doi:10.1016/j.revpalbo.2008.07.007.

Lind BM, Menon M, Bolte CE, Faske TM, Eckert AJ (2018) The genomics of local adaptation in trees: Are we out of the woods yet? *Tree Genetics & Genomes*, **14**, 29.

Martin G, Chapuis E, Goudet J (2008) Multivariate Q_{ST}–F_{ST} comparisons: A neutrality test for the evolution of the G matrix in structured populations. *Genetics*, **180**, 2135–2149. doi: 10.1534/genetics.107.080820.

Mosca E, Eckert AJ, Di Pierro EA, Rocchini D, La Porta N, Belletti P, Neale DB (2012) The geographical and environmental determinants of genetic diversity for four alpine conifers of the European Alps. *Molecular Ecology*, **21**, 5530–5545.

Mousseau TA, Roff DA (1987) Natural selection and the heritability of fitness components. *Heredity*, **59**, 181.

Ovaskainen O, Karhunen M, Zheng C, Arias JMC, Merilä J (2011) A new method to uncover signatures of divergent and stabilizing selection in quantitative traits. *Genetics*, **189**, 621–632. doi:10.1534/genetics.111.129387.

Petit RJ, Hampe A (2006) Some evolutionary consequences of being a tree. *Annu. Rev. Ecol. Evol. Syst.*, **37**, 187–214.

Pigliucci M, Preston KA (2004) *Phenotypic integration: studying the ecology and evolution of complex phenotypes*. Oxford University Press, Oxford, UK.

Pritchard JK, Stephens M, Donnelly PJ (2000) Inference of population structure using multilocus genotype data. *Genetics*, **155**, 945–959.

Roschanski AM, Csilléry K, Liepelt S, *et al.* (2016) Evidence of divergent selection for drought and cold tolerance at landscape and local scales in *Abies alba* mill. in the French Mediterranean Alps. *Molecular Ecology*, **25**, 776–794.

Roschanski AM, Fady B, Ziegenhagen B, Liepelt S (2013) Annotation and re-sequencing of genes from de novo transcriptome assembly of *Abies alba* (*Pinaceae*). *Applications in Plant Sciences*, **1**, 1200179. doi:10.3732/apps.1200179.

Ruosch M, Spahni R, Joos F, Henne PD, van der Knaap WO, Tinner W (2016) Past and future evolution of *Abies alba* forests in Europe - comparison of a dynamic vegetation model with palaeo data and observations. *Global Change Biology*, **22**, 727–740. doi:10.1111/gcb.13075.

Savolainen O, Pyhäjärvi T, Knürr T (2007) Gene Flow and Local Adaptation in Trees. *Annual Review of Ecology, Evolution, and Systematics*, **38**, 595–619. doi:10.1146/annurev.ecolsys.38.091206.095646.

Shaw RG, Etterson JR (2012) Rapid climate change and the rate of adaptation: insight from experimental quantitative genetics. *New Phytologist*, **195**, 752–765.

Stocker TF, Qin D, Plattner GK, *et al.* (2014) *Climate change 2013: The physical science basis*. Cambridge University Press Cambridge, UK, and New York.

Thornton K (2003) libsequence: A C++ class library for evolutionary genetic analysis. *Bioinformatics*, **19**, 2325–2327. doi:10.1093/bioinformatics/btg316.

Van der Knaap W, van Leeuwen JF, Finsinger W, *et al.* (2005) Migration and population expansion of *Abies*, *Fagus*, *Picea*, and *Quercus* since 15000 years in and across the Alps, based on pollen-percentage threshold values. *Quaternary Science Reviews*, **24**, 645–680.

Vilella AJ, Blanco-Garcia A, Hutter S, Rozas J (2005) VariScan: analysis of evolutionary patterns from large-scale DNA sequence polymorphism data. *Bioinformatics*, **21**, 2791–2793.

Visscher PM, Hill WG, Wray NR (2008) Heritability in the genomics era - concepts and misconceptions. *Nature Reviews Genetics*, **9**, 255–266. doi:10.1038/nrg2322.

Vitali V, Büntgen U, Bauhus J (2017) Silver fir and Douglas fir are more tolerant to extreme droughts than Norway spruce in south-western Germany. *Global Change Biology*. doi: 10.1111/gcb.13774.

Waitt DE, Levin DA (1998) Genetic and phenotypic correlations in plants: a botanical test of cheverud's conjecture. *Heredity*, **80**, 310–319.

Wells N, Goddard S, Hayes MJ (2004) A self-calibrating Palmer drought severity index. *Journal of Climate*, **17**, 2335–2351. doi:10.1175/1520-0442(2004)017<2335:ASPDSI>2.0.CO;2.

Whitlock MC (2008) Evolutionary inference from q_{ST}. *Molecular Ecology*, **17**, 1885–1896.

Whitlock MC, Guillaume F (2009) Testing for spatially divergent selection: comparing q_{ST} to f_{ST}. *Genetics*, **183**, 1055–1063.

Yeaman S, Hodgins KA, Lotterhos KE, *et al.* (2016) Convergent local adaptation to climate in distantly related conifers. *Science*, **353**, 1431–1433.

Tables

Table 1: Climatic variables developed in this study using statistical downscaling from Chelsa (Karger *et al.*, 2017) and the CRU TS v. 4.01 data (Harris *et al.*, 2014). Monthly mean, minimum and maximum temperature and total precipitation were used to calculate the bioclimatic, PET, SPEI and frost variables. Soil AWC was extracted from the SoilGrids data base (Hengl *et al.*, 2017), and used for the calculation of the scPDSI variables.

Variable	Description	Mean	(Min., Max.)
Standard Bioclimaic variables			
bio.1	Annual Mean Temperature	6.1	$(3.1, 9.3)$
bio.2	Mean Diurnal Range (Mean of monthly Tmax - Tmin))	8.9	$(8.6, 9.2)$
bio.3	Isothermality (bio.2/bio.7) (* 100)	23.9	$(23.2, 24.6)$
bio.4	Temperature Seasonality (standard deviation *100)	663.7	$(636.4, 676.9)$
bio.5	Max Temperature of Warmest Month	24.2	$(21, 27.4)$
bio.6	Min Temperature of Coldest Month	-13	$(-15.8, -10)$
bio.7	Temperature Annual Range (bio.5-bio.6)	37.2	$(36.2, 37.9)$
bio.8	Mean Temperature of Wettest Quarter	9.5	$(-2.6, 17.7)$
bio.9	Mean Temperature of Driest Quarter	-1.7	$(-6.1, 3.9)$
bio.10	Mean Temperature of Warmest Quarter	16.8	$(13.8, 20)$
bio.11	Mean Temperature of Coldest Quarter	-6	$(-8.5, -3.3)$
bio.12	Annual Precipitation	1176.4	$(505.6, 1690.9)$
bio.13	Precipitation of Wettest Month	281	$(128.1, 432.6)$
bio.14	Precipitation of Driest Month	4	$(0.4, 9.1)$
bio.15	Precipitation Seasonality (Coefficient of Variation)	50	$(46, 55.3)$
bio.16	Precipitation of Wettest Quarter	641.2	$(274.2, 1024.7)$
bio.17	Precipitation of Driest Quarter	55.6	$(24.5, 83.7)$
bio.18	Precipitation of Warmest Quarter	277.3	$(156, 442.9)$
bio.19	Precipitation of Coldest Quarter	222.7	$(65.6, 452.7)$
Soil			
AWC	Available Water Capacity (SoilGrids data base)	163.9	$(147.7, 184.5)$
Potential Evapotranspiration (PET)			
PET.thorn	Mean annual Potential Evapotranspiration (Thornthwaite)	43.8	$(37.3, 51.8)$
PET.harg	Mean annual n (Hargreaves)	52.6	$(47.3, 59.4)$
Standardised Precipitation-Evapotranspiration Index (SPEI)			
SPEI.m1	Number of month with SPEI < -1	162	$(144, 178)$
SPEI.m2	Number of month with SPEI < -2	13.8	$(7, 22)$
SPEI.q5	The 5% quantile of SPEI	-1.6	$(-1.6, -1.5)$
SPEI.q1	The 1% quantile of SPEI	-2.1	$(-2.2, -1.9)$
self-calibrated Palmer's Drought Severity Index (scPDSI)			
scPDSI.m3	Number of month with scPDSI < -3	42.6	$(29, 53)$
scPDSI.m4	Number of month with scPDSI < -4	9.6	$(2, 14)$
scPDSI.q5	The 5% quantile of scPDSI	-3.2	$(-3.4, -2.8)$
scPDSI.q1	The 1% quantile of scPDSI	-4.5	$(-4.9, -4.1)$
Late frost			
late.frost	Min temperature of the first month of the year with mean temperature $> 5°\mathrm{C}$	1.7	$(1.4, 2)$
late.frost2	Min temperature of May	4.7	$(1.5, 8.2)$

Table 2: Summary of single trait tests of adaptive divergence. Q_{ST}, $Q_{ST} - F_{ST}$ and p-value correspond to the Whitlock & Guillaume (2009) approach, S is the summary of evidence of selection using the Ovaskainen *et al.* (2011) method, H indicates the role of the environment in adaptation using the Karhunen *et al.* (2014) test, and H^* is a standardized version of H proposed in the study. Both H and H^* were calculated with all environmental variables listed in Tables 1 and S1. S, H, and H^* values close to one indicate high evidence of divergent selection.

Trait	Q_{ST}	Q_{ST}-F_{ST}	p-value	S statistic	H statistic	H^* statistic
Diameter	0.082	0.076	0.032	0.953	0.971	0.883
Height	0.268	0.262	0.001	1.000	1.000	0.930
Height/Diameter	0.245	0.239	0.045	0.864	0.449	0.606
Growth Rate	0.060	0.054	0.113	0.768	0.828	0.703
Growth Duration	0.275	0.269	0.031	0.944	0.905	0.473
Terminal Bud Break	0.212	0.206	0.020	0.958	0.880	0.534
Lateral Bud Break	0.138	0.132	0.016	0.964	0.885	0.480
Growth Cessation	0.436	0.430	0.045	0.551	0.425	0.355

Figure legends

Figure 1. A: Geographic situation of the sampling sites. B: Drift distances between populations as estimated with the admixture F-model (AFM). The mean coancestry between populations is averaged over the 10 independent Markov chains, from which distances were calculated to draw the dendrogram.

Figure 2. Summary of the single-trait test of adaptive divergence using the Ovaskainen *et al.* (2011) method for the eight studied traits shown across panels A to H. Each panel shows the ancestral additive mean trait value (horizontal line), the amount of trait divergence from this mean that is expected based on drift (gray envelop), and the estimated posterior distribution of the additive trait values for each population (boxes). A star above the boxes indicates a significant population-wise S test. Population order is different on each panel since populations are ordered according to their additive trait values.

Figure 3. Summary of the two-trait analysis of adaptive divergence using the Ovaskainen *et al.* (2011) method. Panel A shows the phenotypic (r_p) and genetic (r_g) correlations between trait pairs (see main text for formula). The top three trait pairs with $r_p \geq r_g$ are highlighted in gray, and those with $r_g \geq r_p$ in black. Panel B shows the S statistic for the two-trait selection test as a function of r_g. The three traits pairs with $r_g > r_p$ highlighted in panel A are also highlighted here.

Figure 4. Correlated adaptive divergence in Height and Diameter using the Ovaskainen *et al.* (2011) method. Ellipses represent the median amount of trait divergence that is expected based on drift for each population. Population names (3 letters) represent the median of the posterior distribution of the additive trait values for each population. Ellipses and population names with a significant trait divergence are shown in black, while populations that do not deviate from the drift are in gray.

Figure 5. Correlated adaptive divergence at Terminal Bud Break, Growth Duration and Growth Rate using the Ovaskainen *et al.* (2011) method. Each panel shows the evidence for unusual trait divergence in a two trait space. Ellipses represent the median amount of trait divergence that is expected based on drift for each population. Population names (3 letters) represent the median of the posterior distribution of the additive trait values for each population. Ellipses and population names with a significant trait divergence are shown in black, while populations that do not deviate from the drift are in gray.

Figure 6. Comparison of the H and H^* statistics for the eight studied traits to assess the role of the environment in explaining trait divergence. Each point indicated the H and H^* statistics for a trait (see symbols) and an environmental variable listed in Tables 1 and SS1.

Figure 7. A: The first two principal components of the environmental variables that had a H^* statistics higher than 0.95 for Height and Diameter. Populations that showed a signature of adaptive divergence for Height in the population-wise S-test are situated in the "warm" and "stable", left-side of the environmental space and are indicated by bigger latter sizes for their population code (for clarity, these are VWD, BEI, COR, LUT, SIG, GRB, MGY, MUO). B: The first two principal components of the environmental variables that had and H^* statistics higher than 0.85 for Growth Rate and Duration, and Terminal and Lateral Bud Break. Populations that showed a signature of adaptive divergence for these traits in the single or multi-trait population-wise S-test are indicated by bigger latter sizes for their population code (for clarity, these are SIR, MGY, VRG). Explications of the environmental axes (in gray) can be found in Table 1.

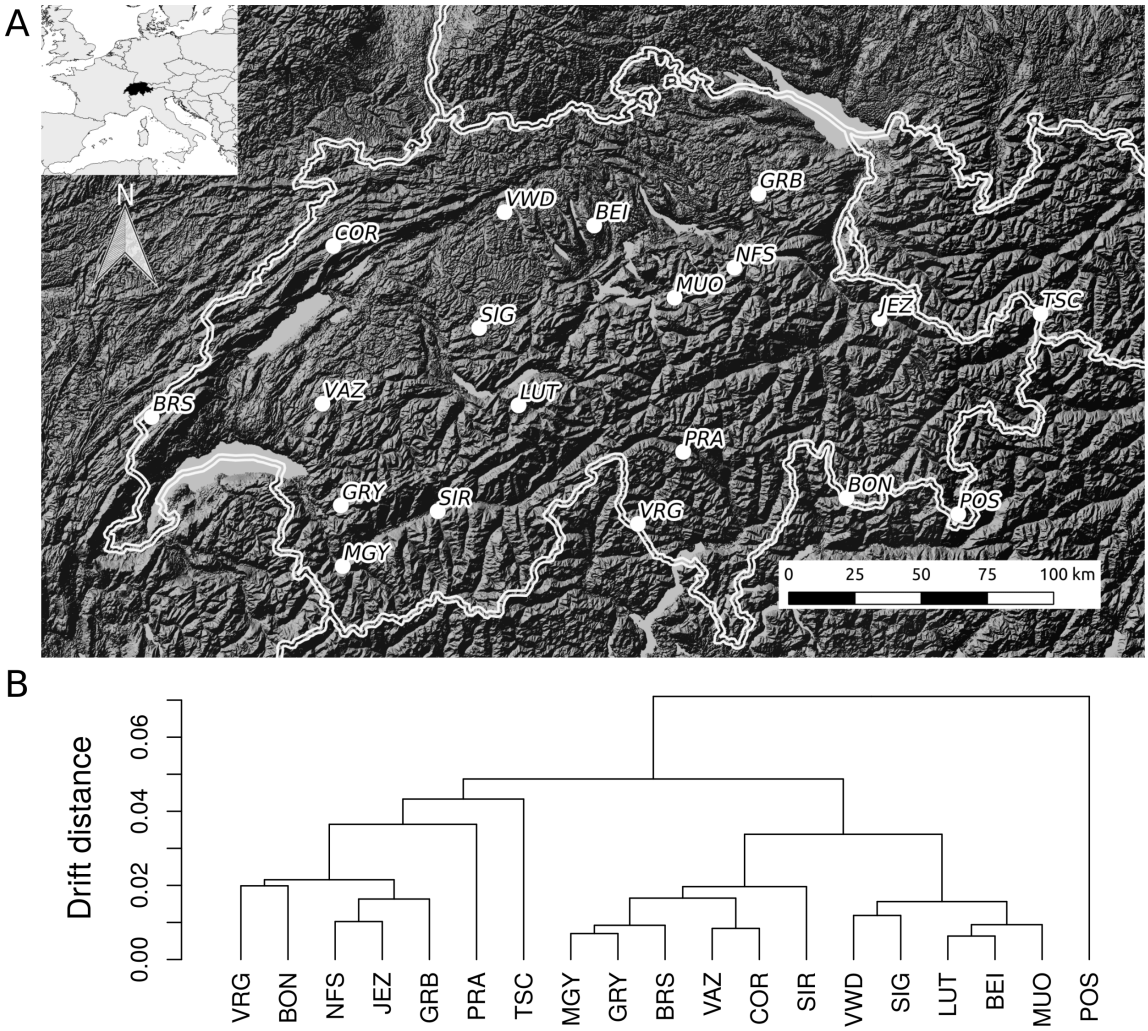
A
N
GRB
VWD
BEI
COR
NFS
MUO
JEZ
TSC
SIG
BRS
VAZ
LUT
PRA
BON
POS
GRY
SIR
VRG
MGY
0 25 50 75 100 km
B
Drift distance
0.00
0.02
0.04
0.06
VRG
BON
NFS
JEZ
GRB
PRA
TSC
MGY
GRY
BRS
VAZ
COR
SIR
VWD
SIG
LUT
BEI
MUO
POS

Figure 1

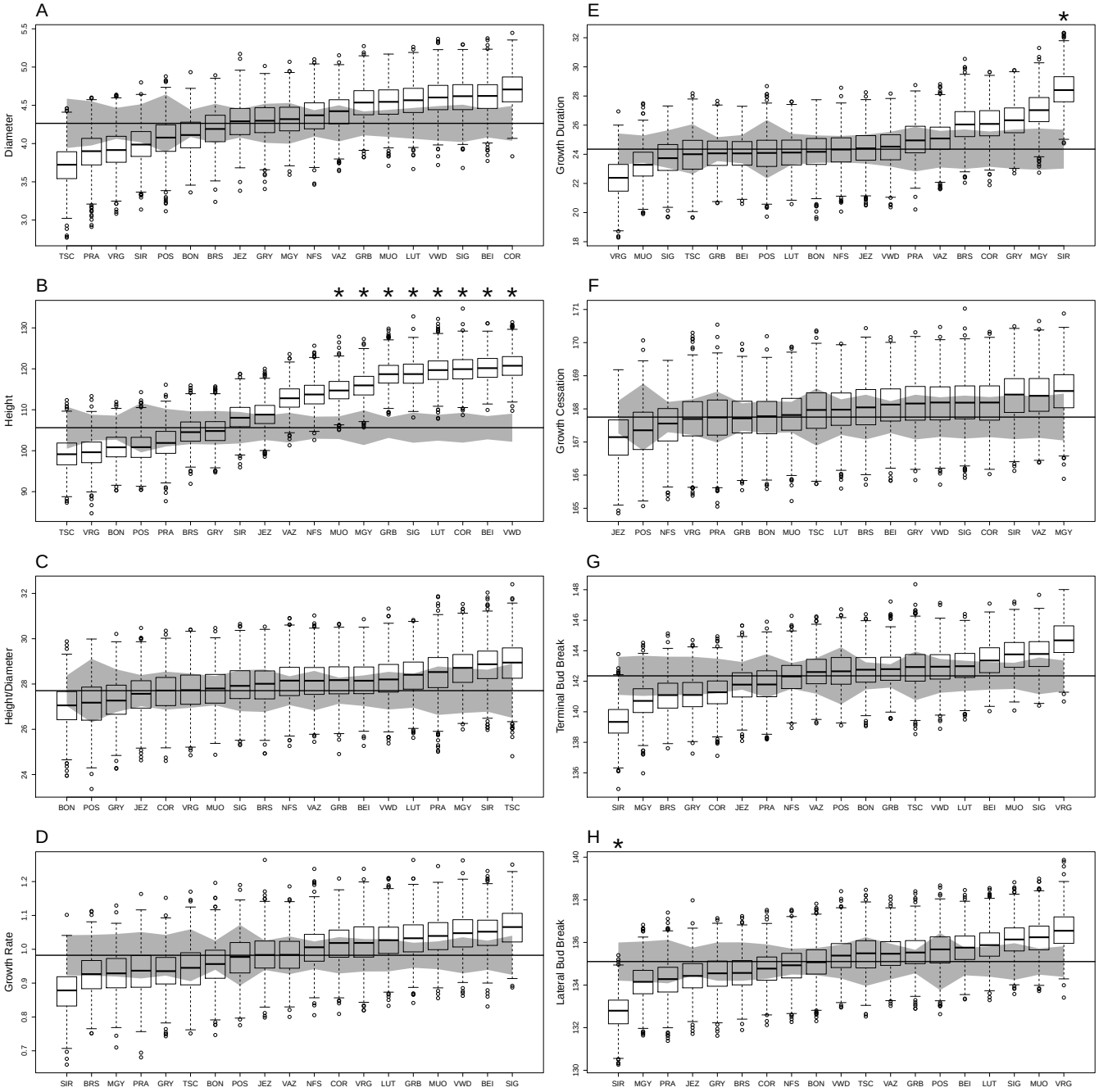
A
Diameter
TSC PRA VRG SIR POS BON BRS JEZ GRY MGY NFS VAZ GRB MUO LUT VWD SIG BEI COR
B
Height
TSC VRG BON POS PRA BRS GRY SIR JEZ VAZ NFS MUO MGY GRB SIG LUT COR BEI VWD
C
Height/Diameter
BON POS GRY JEZ COR VRG MUO SIG BRS NFS VAZ GRB BEI VWD LUT PRA MGY SIR TSC
D
Growth Rate
SIR BRS MGY PRA GRY TSC BON POS JEZ VAZ NFS COR VRG LUT GRB MUO VWD BEI SIG
E
Growth Duration
VRG MUO SIG TSC GRB BEI POS LUT BON NFS JEZ VWD PRA VAZ BRS COR GRY MGY SIR
F
Growth Cessation
JEZ POS NFS VRG PRA GRB BON MUO TSC LUT BRS BEI GRY VWD SIG COR SIR VAZ MGY
G
Terminal Bud Break
SIR MGY BRS GRY COR JEZ PRA NFS VAZ POS BON GRB TSC VWD LUT BEI MUO SIG VRG
H
Lateral Bud Break
SIR MGY PRA JEZ GRY BRS COR NFS BON VWD TSC VAZ GRB POS BEI LUT SIG MUO VRG

Figure 2

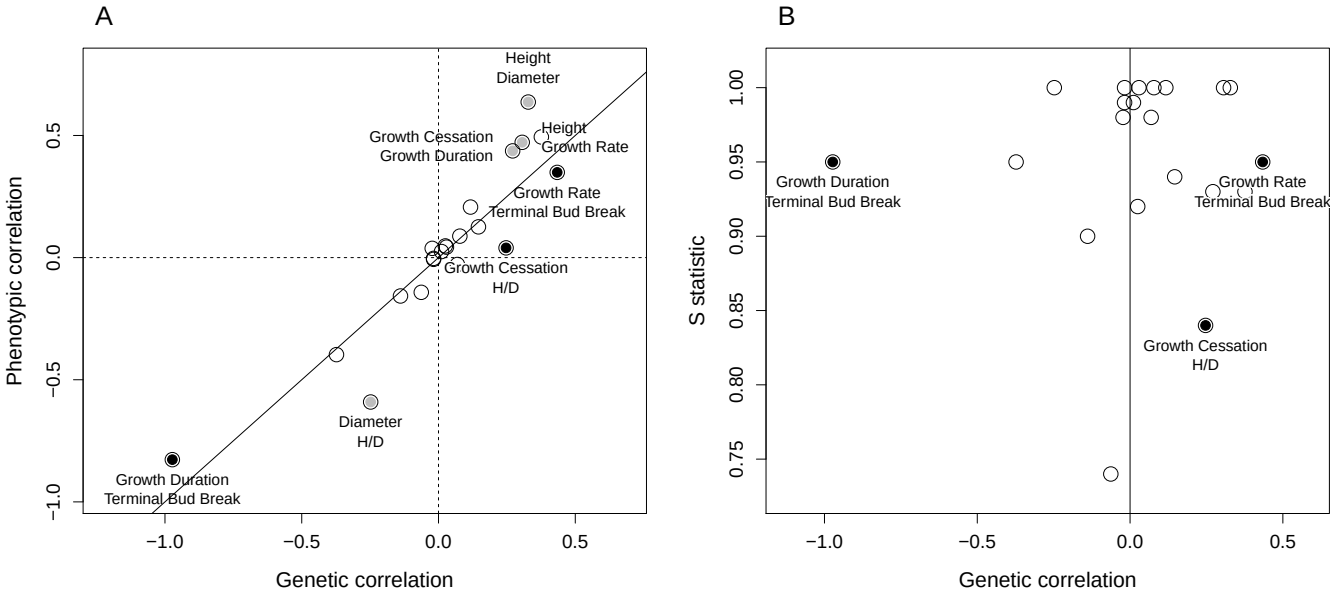
A
Height
Diameter
Height
Growth Rate
Growth Cessation
Growth Duration
Growth Rate
Terminal Bud Break
Growth Cessation
H/D
Diameter
H/D
Growth Duration
Terminal Bud Break
Phenotypic correlation
Genetic correlation
B
Growth Duration
Terminal Bud Break
Growth Rate
Terminal Bud Break
Growth Cessation
H/D
S statistic
Genetic correlation

Figure 3

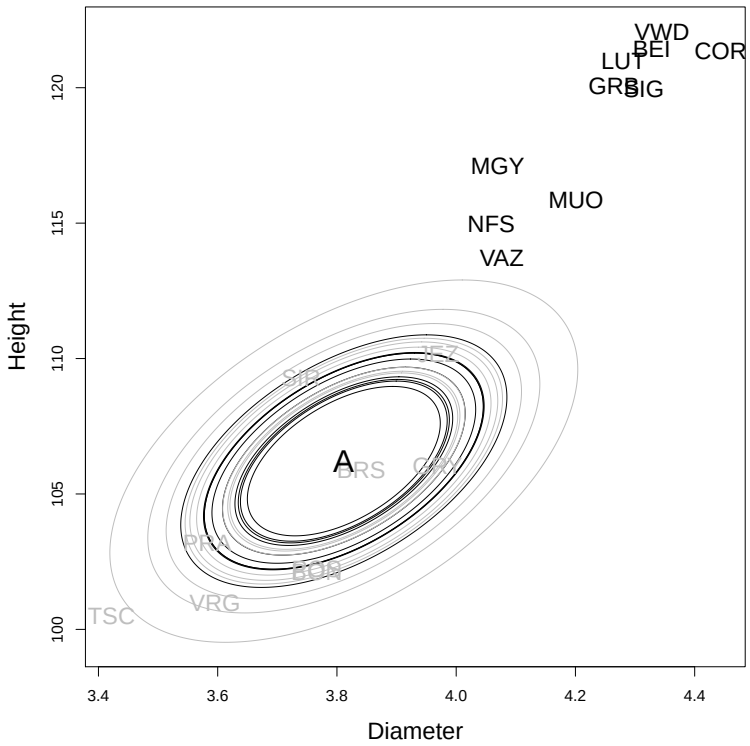
VWD
BEI
COR
LUT
GRB
SIG
MGY
MUO
NFS
VAZ
JEZ
SID
A
BRS
GRY
PRA
BOR
VRG
TSC
Height
Diameter
100
105
110
115
120
3.4
3.6
3.8
4.0
4.2
4.4

Figure 4

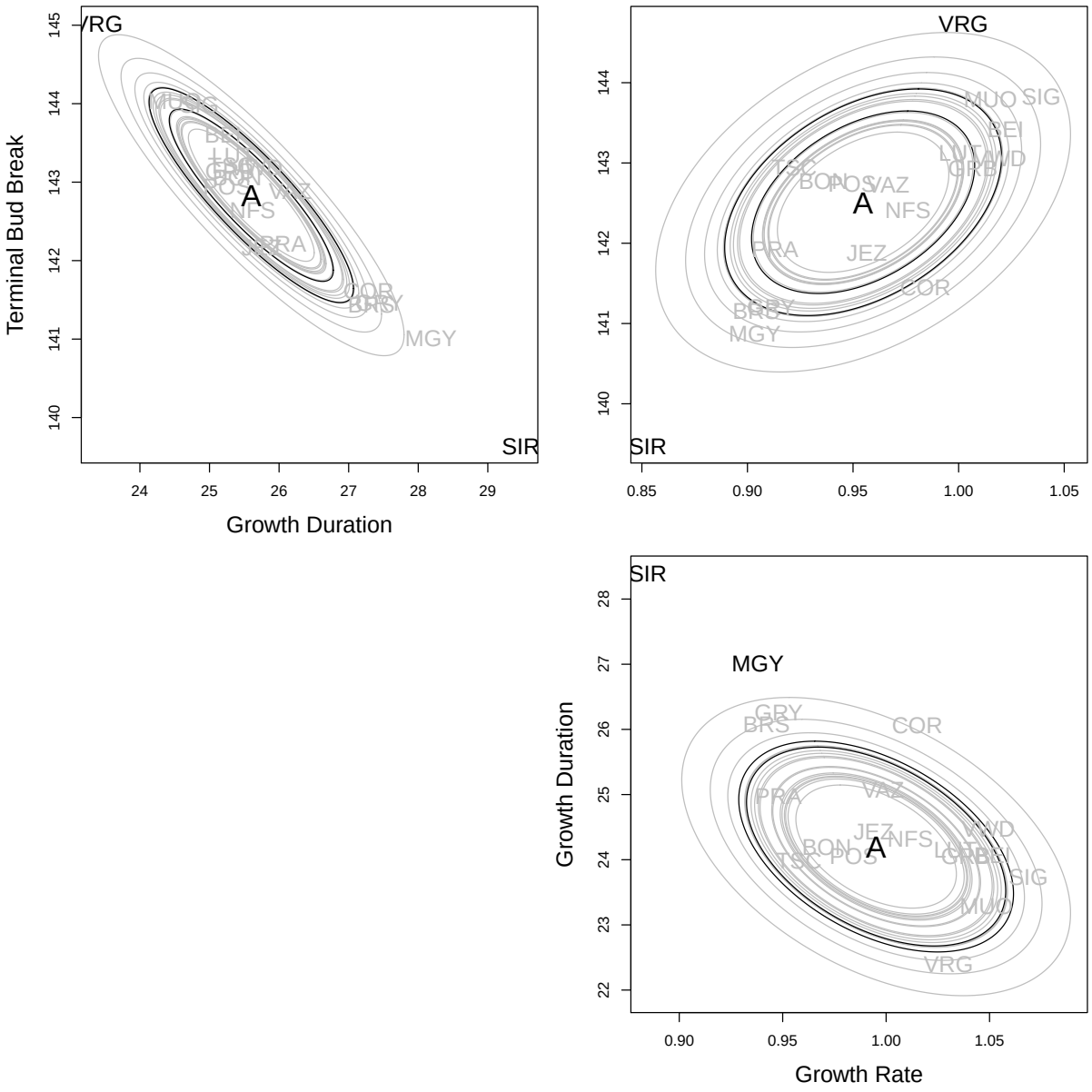
VRG
SIR
A
MGY
Terminal Bud Break
Growth Duration
Growth Rate
145
144
143
142
141
140
24
25
26
27
28
29
0.85
0.90
0.95
1.00
1.05
27
26
25
24
23
22
MUO
SIG
SEI
LUT
WD
GRB
TSC
BON
POS
VAZ
NFS
PRA
JEZ
COR
GRY
BRS

Figure 5

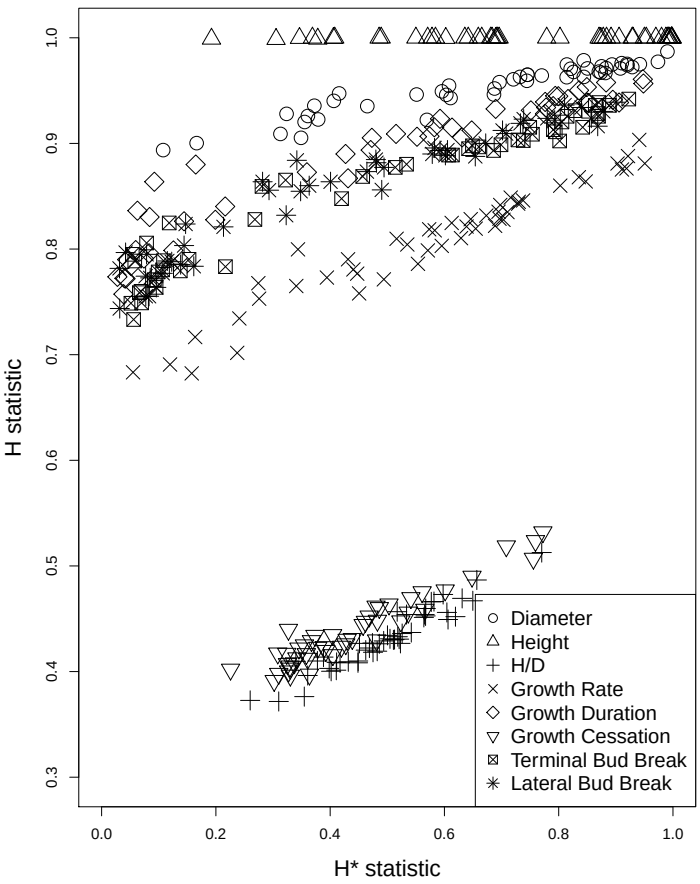
H statistic
H* statistic
0.3
0.4
0.5
0.6
0.7
0.8
0.9
1.0
0.0
0.2
0.4
0.6
0.8
1.0
Diameter
Height
H/D
Growth Rate
Growth Duration
Growth Cessation
Terminal Bud Break
Lateral Bud Break

Figure 6

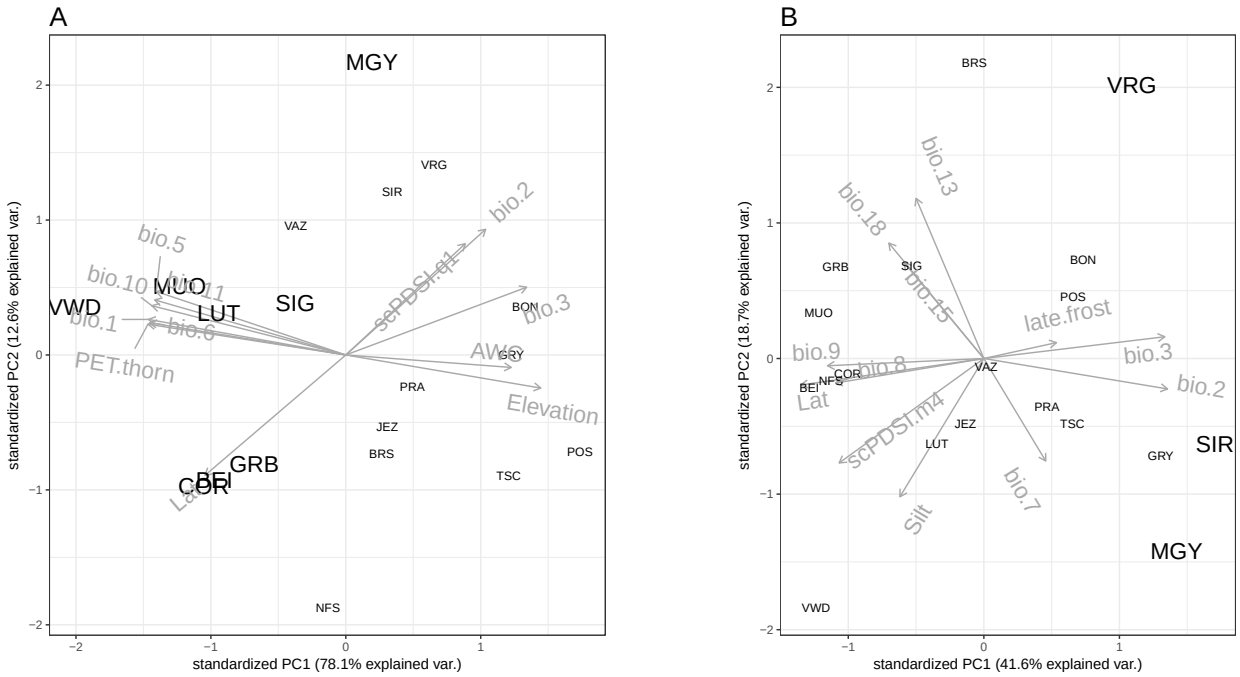
A
MGY
VRG
SIR
VAZ
bio.2
bio.5
bio.10
bio.11
MUO
VWD
LUT
SIG
scPDSI.q1
BON
bio.3
bio.1
bio.6
AWC
GRY
PET.thorn
PRA
Elevation
JEZ
BRS
POS
GRB
BEI
COR
Lat
TSC
NFS
standardized PC2 (12.6% explained var.)
standardized PC1 (78.1% explained var.)
B
BRS
VRG
bio.13
bio.18
GRB
SIG
BON
bio.15
POS
MUO
late.frost
bio.9
bio.3
bio.8
VAZ
COR
NFS
BEI
bio.2
Lat
PRA
TSC
JEZ
scPDSI.m4
LUT
SIR
GRY
bio.7
Silt
MGY
VWD
standardized PC2 (18.7% explained var.)
standardized PC1 (41.6% explained var.)

Figure 7

Supplementary Tables

Table S1: Geography and soil variables from local soil pits as described in (Frank *et al.*, 2017b).

Variable	Description	Mean	(Min., Max.)
Geography			
Long	Longitude (degrees)	8.3	$(6.2, 10.5)$
Lat	Latitude (degrees)	46.7	$(46.1, 47.3)$
Elev	Elevation (m a.s.l)	1062.2	$(481, 1602.5)$
Slope	Slope (%)	40	$(0, 70)$
Local soil pits			
Sand	Sand content of lower soil (ca. 45-55 cm)	43	$(12.6, 89.2)$
Silt	Silt content of lower soil (ca. 45-55 cm)	36.3	$(8.3, 63.2)$
Clay	Clay content of lower soil (ca. 45-55 cm)	20.6	$(2.5, 66.8)$
N.tot	Total N of top soil layer (ca. 5-15 cm)	0.3	$(0.1, 1.2)$
C.tot	Total C of top soil layer (ca. 5-15 cm)	5.6	$(1, 18.8)$
C.org	Organic C of top soil layer (ca. 5-15 cm)	5.4	$(1, 17.9)$
pH	pH of top soil layer (ca. 5-15 cm)	5.1	$(3.4, 7.5)$
AC.1m	Air capacity of 1 m soil depth	112.3	$(36.8, 209.4)$
AWC.1m	Available water capacity of 1 m soil depth	139.5	$(31.5, 229.4)$

Table S2: Heritability (h^2) and genetic correlation (r_g) from the multi-trait analysis using the Ovaskainen *et al.* (2011) method. r_p is the Person correlation between the two traits using the raw data.

Trait pair	h_1^2	h_2^2	r_g	r_p
Height-Diameter	0.565	0.672	0.328	0.637
Height-Height/Diameter	0.564	0.751	0.117	0.207
Height-Growth Rate	0.560	0.646	0.306	0.472
Height-Growth Duration	0.581	0.918	−0.018	−0.007
Height-Terminal Bud Break	0.570	0.813	0.029	0.043
Height-Growth Cessation	0.568	0.430	0.078	0.088
Diameter-Height/Diameter	0.797	0.746	−0.248	−0.592
Diameter-Growth Rate	0.886	0.699	0.376	0.494
Diameter-Growth Duration	0.871	0.790	0.011	0.025
Diameter-Terminal Bud Break	0.891	0.821	−0.018	−0.003
Diameter-Growth Cessation	0.883	0.534	0.025	0.048
Height/Diameter-Growth Rate	0.781	0.755	−0.139	−0.157
Height/Diameter-Growth Duration	0.720	0.754	0.069	−0.028
Height/Diameter-Terminal Bud Break	0.777	0.801	−0.023	0.038
Height/Diameter-Growth Cessation	0.678	0.420	0.247	0.040
Growth Rate-Growth Duration	0.802	0.649	−0.373	−0.397
Growth Rate-Terminal Bud Break	0.711	0.807	0.434	0.349
Growth Rate-Growth Cessation	0.740	0.484	−0.063	−0.142
Growth Duration-Terminal Bud Break	0.738	0.753	−0.973	−0.827
Growth Duration-Growth Cessation	0.762	0.480	0.271	0.437
Terminal Bud Break-Growth Cessation	0.819	0.607	0.146	0.126

Supplementary figures

Figure S1. Correlations between trait values (lower triangle), the distribution of trait values (diagonal), and Pearson's correlation coefficient and p-values from a correlation test (upper triangle).

Figure S2. Situation of the 19 population locations in along the first four Principal Components of all environmental variables listed in Table 1 and S1 centered and scaled.

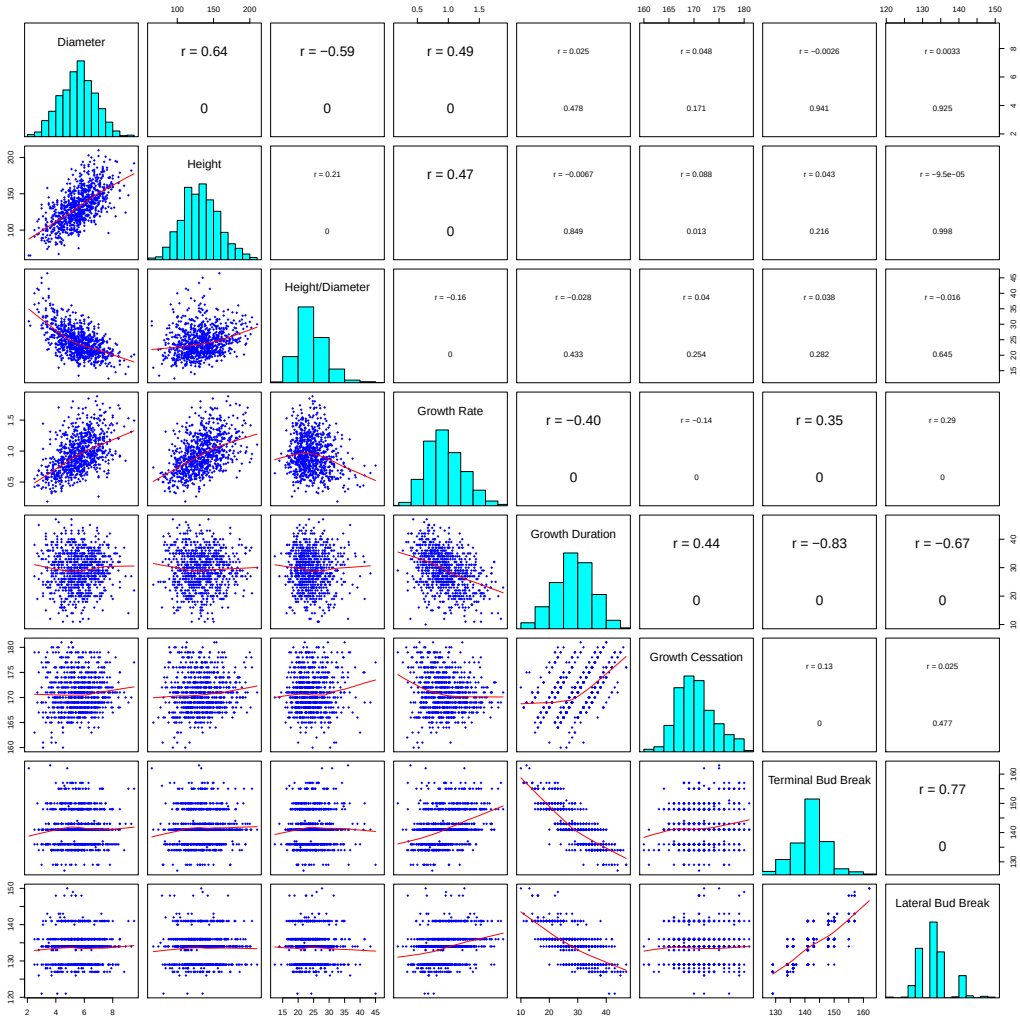
Diameter
r = 0.64
0
r = −0.59
0
r = 0.49
0
r = 0.025
0.478
r = 0.048
0.171
r = −0.0026
0.941
r = 0.0033
0.925
Height
r = 0.21
0
r = 0.47
0
r = −0.0067
0.849
r = 0.088
0.013
r = 0.043
0.216
r = −9.5e−05
0.998
Height/Diameter
r = −0.16
0
r = −0.028
0.433
r = 0.04
0.254
r = 0.038
0.282
r = −0.016
0.645
Growth Rate
r = −0.40
0
r = −0.14
0
r = 0.35
0
r = 0.29
0
Growth Duration
r = 0.44
0
r = −0.83
0
r = −0.67
0
Growth Cessation
r = 0.13
0
r = 0.025
0.477
Terminal Bud Break
r = 0.77
0
Lateral Bud Break

Figure S1

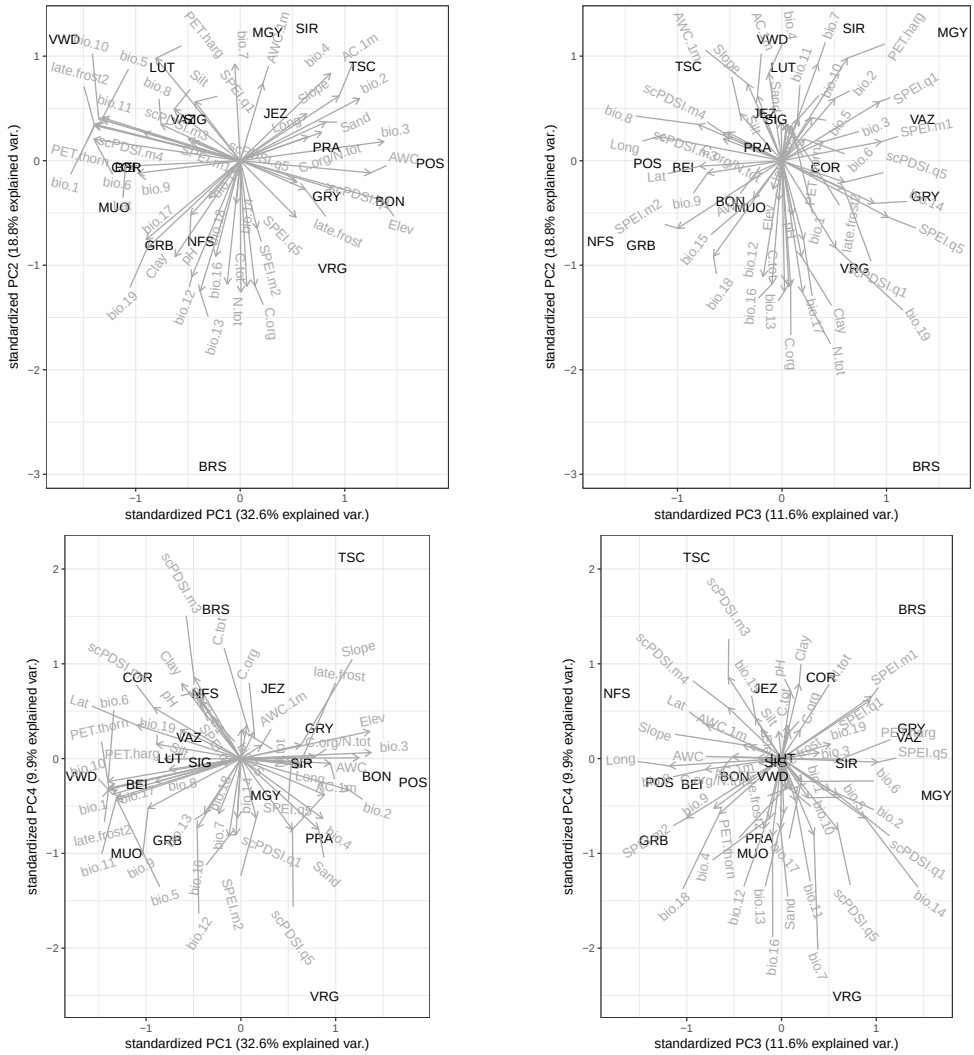
standardized PC1 (32.6% explained var.)
standardized PC2 (18.8% explained var.)
standardized PC3 (11.6% explained var.)
standardized PC4 (9.9% explained var.)
VWD
MGY
SIR
LUT
TSC
JEZ
VAZ
SIG
PRA
POS
COR
GRY
BON
MUO
GRB
NFS
VRG
BRS
BEI

Figure S2

Contrasting population structure using AFM and Structure

To further validate the results of the AFM model, we used the Bayesian clustering algorithm implemented in Structure v.2.3.4 Pritchard *et al.* (2000) to cluster individuals to K groups. Neither AFM nor Structure is "better", so our objective was simply to compare if the two algorithms provide similar results. We used the admixture model with correlated allele frequencies Falush *et al.* (2003), which is the closest model to AFM. Further, we included sampling location information to improve clustering performance ("locprior model", Hubisz *et al.* (2009)), an additional information that cannot be accounted for in AFM. We estimated the prior population allele frequency parameter (λ) from the data, as the default of 1 is not necessarily a good choice for SNP data, where most minor alleles are rare. We estimated λ using K = 1 to avoid non-identifiability issues with the other hyper-parameters (λ, α, F). λ was consistently around 0.65 across ten repeated runs (range: 0.63-0.66, median: 0.65). Then, we tested K values from 1 to 19 using ten independent Markov chains for each K, and 500,000 burn-in iterations and 500,000 iterations for estimation of the membership coefficients. Different number of clusters (K) were compared with StructureHarvester (Earl *et al.*, 2012) using the $LnPr(X|K)$ and Evanno *et al.*'s (2005) method. Admixture coefficients were averaged across ten repeated runs using CLUMPP v.1.1.2 Jakobsson & Rosenberg (2007) using the Greedy algorithm for any K>3 and large-K-Greedy for K>5.

Structure and AFM results were compared for each K using a Mantel test (ecodist R package). We calculated a distance matrix from the coancestry matrix and compared to a distance matrix calculated from the CLUMPP outfiles for each K. The individual coancestries of the CLUMPP outfiles were first reduced to population coancestries by taking the mean coancestry of the individuals within a population for each K yielding a 19 $\times$ K matrix for $K = 2, \therefore, 19$. Dendrograms from AFM and Structure were also compared visually using the dendextend R package (Galili, 2015).

The software Structure using the log likelihood criteria suggested five as optimal number of clusters, nevertheless, additional increase in the log likelihood is suggestive of deeper hierarchical structure (Figure A1). The highest similarity between AFM and Structure was

achieved for $K = 4$ (Figure A2 and A3). Structure also generally confirmed the east-west differentiation as first level structure and several parts of the dendrograms from the two algorithms were identical (Figure A3). We concluded that AFM gave reliable, and most likely more precise results in comparison to Structure.

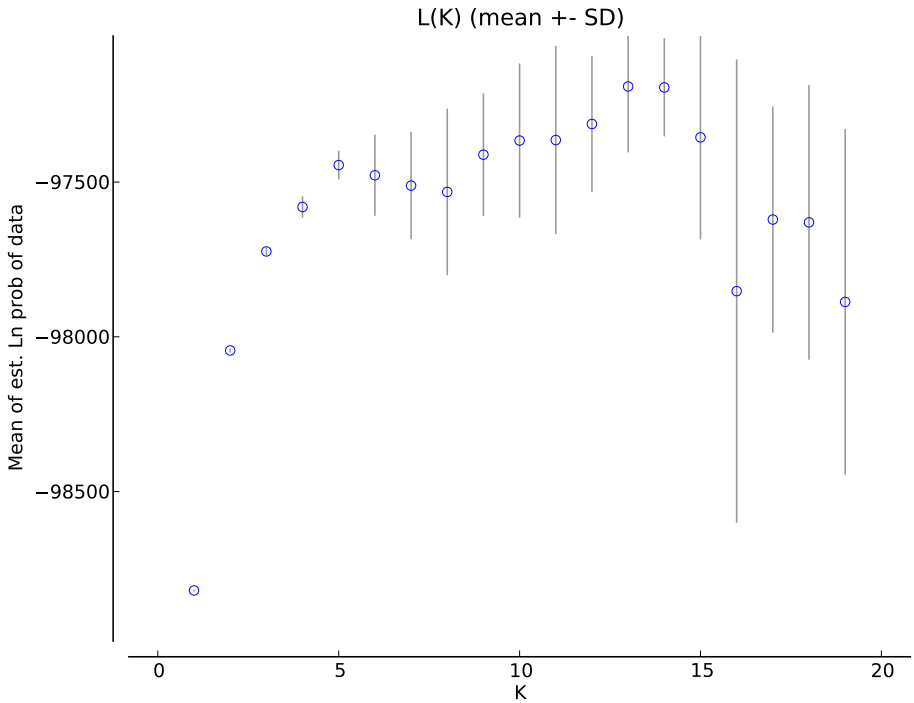

Figure A1: The log-likelihood from Structure from $K = 2$ to 19.

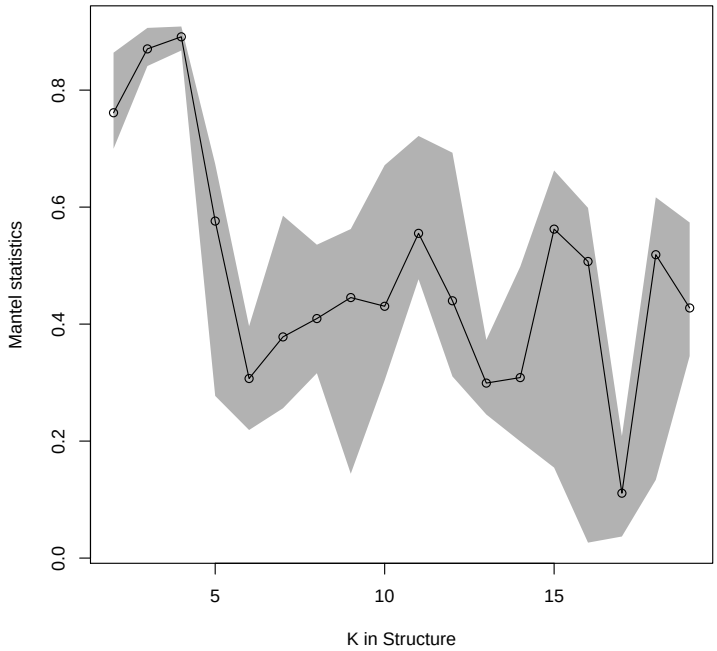

Figure A2: Mantel test statistic and its 95% percentile interval from a randomization procedure between distance matrices from AFM and Structure from $K = 2$ to 19.

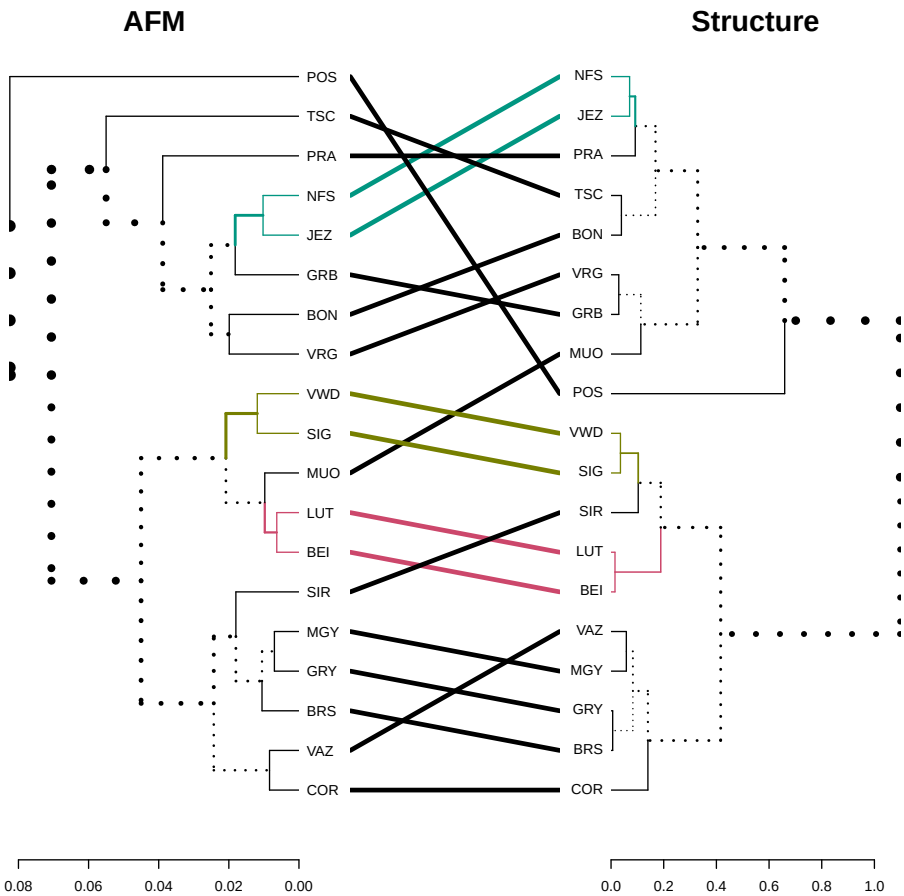

Figure A3: Entangled dendrograms from AFM and Structure with $K = 4$.